Korea-Australia Rheology Journal, Vol.27, No.1, pp.1-10 (February 2015) www.springer.com/13367
DOI: 10.1007/s13367-015-0001-4

Effect of cholesterol and triglycerides levels on the rheological behavior of human blood

Leonardo Moreno[1], Fausto Calderas[1,*], Guadalupe Sanchez-Olivares[2], Luis Medina-Torres[3], Antonio Sanchez-Solis[1] and Octavio Manero[1]

[1]*Instituto de Investigaciones en Materiales, Universidad Nacional Autónoma de México, A.P. 70-360, México, D.F., 04510*
[2]*CIATEC, A.C. Omega 201, Industrial Delta, CP 37545, León, Gto, Mexico*
[3]*Departamento de Ingeniería Química, Facultad de Química, UNAM*

(Received May 29, 2014; final revision received January 5, 2015; accepted January 8, 2015)

Important public health problems worldwide such as obesity, diabetes, hyperlipidemia and coronary diseases are quite common. These problems arise from numerous factors, such as hyper-caloric diets, sedentary habits and other epigenetic factors. With respect to Mexico, the population reference values of total cholesterol in plasma are around 200 mg/dL. However, a large proportion has higher levels than this reference value. In this work, we analyze the rheological properties of human blood obtained from 20 donors, as a function of cholesterol and triglyceride levels, upon a protocol previously approved by the health authorities. Samples with high and low cholesterol and triglyceride levels were selected and analyzed by simple-continuous and linear-oscillatory shear flow. Rheometric properties were measured and related to the structure and composition of human blood. In addition, rheometric data were modeled by using several constitutive equations: Bautista-Manero-Puig (BMP) and the multimodal Maxwell equations to predict the flow behavior of human blood. Finally, a comparison was made among various models, namely, the BMP, Carreau and Quemada equations for simple shear rate flow. An important relationship was found between cholesterol, triglycerides and the structure of human blood. Results show that blood with high cholesterol levels (400 mg/dL) has flow properties fully different (higher viscosity and a more pseudo-plastic behavior) than blood with lower levels of cholesterol (tendency to Newtonian behavior or viscosity plateau at low shear rates).

***Keywords*:** blood rheology, cholesterol, triglycerides, BMP constitutive equation

1. Introduction

The existence of highly-developed multicellular organisms is unthinkable without an adequate blood supply to the tissues. Blood carries and removes gases, nutrients, metabolites and heat from the tissues. Human blood is a complex, non-Newtonian fluid, which flows in most tissues of the human body. It is a suspension of red cells in a liquid (plasma) (Schmid-Schönbein *et al*., 1968); the latter is composed of water, inorganic ions, hormones, glucose and proteins and amounts to 55% of the whole blood. Erythrocytes are the main cells of human blood with contents of 40-50 vol.% in males, 36-44 vol.% in females (Esteridge *et al*., 2000). Red blood cells dictate the rheological behavior of human blood due to their high content. Among other components, the cholesterol concentration influences the level of transient interactions among cells.

Flow properties are affected by arrangement, orientation and deformability of blood cells (Thurston, 1972; 1975). Human blood exhibits a shear thinning behavior arising from the disruption by flow of weak cell aggregations. These aggregations are transient structures formed by red blood cells which build-up and break-down according to the flow strength. Aggregation of blood cells is promoted by the cholesterol macromolecules, which generate "bridges" between membranes reducing the natural electrostatic repulsion between cells.

Overall blood flow is a complex combination of various flows, including simple shear and pulsatile in oscillating diameter channels (arteries and veins) through the cardiovascular system. Several transient structures undergo a process of formation and deformation within the blood flow. To facilitate the understanding to predict blood flow behavior, it is convenient to analyze the blood under rheometric-controlled flows. The main objective of this paper is to provide further understanding of the flow behavior of blood by analyzing the effect of total cholesterol (TC) and triglycerides (TG) content on the rheology of human blood.

1.1. Samples of human blood

Samples were obtained from 20 donors in the National Institute of Cardiology from research protocols of dyslipidemia and other metabolic disorders. Blood was extracted by venous puncture and later stored in tubes with EDTA (Ethylenediaminetetraacetic acid) to avoid coagulation effects. Analysis was performed with 20 samples of human blood with different levels of total cholesterol, tri-

*Corresponding author: faustocg@unam.mx

glycerides, fibrinogen *etc.* but we selected just 12 samples for graphics in this paper. Most of the samples obtained for this study had moderate concentrations of total cholesterol, triglycerides, and fibrinogen. Therefore, there are larger number of samples with moderate rather than extreme cholesterol contents. These samples have no significant differences in the hematocrit level (the average value between samples is 42 ± 2%). Two tubes of 5 mL for each patient were collected. The first tube was used for biochemical determinations of total cholesterol and triglycerides (the kit used is from Biosystem® Clinical Reagents). The second tube kept the samples for rheological measurements, which were readily performed during the first few minutes after extraction. Stored red cells undergo changes in their shape, deformability and in their hemoglobin function, taking several hours to return to normal conditions following transfusion (Hogman, 1999; Hogman and Meryman, 1999; Longster *et al*., 1972). The most representative samples were chosen for mathematical modeling (20 samples were analyzed), since in most cases samples had similar plasmatic levels of total cholesterol and triglycerides and total proteins. Table 1 summarizes the clinical data for selected blood samples under study. Samples H1-H6 have high cholesterol levels and samples L1-L6 lie within the average range (Lerman-Garber *et al*., 1993).

Triglycerides content in blood is associated with cholesterol content, in as much as high cholesterol levels are accompanied with high plasmatic concentration of triglycerides. Nonetheless, this relationship is not entirely linear and may be modified by various diseases (diabetes, obesity, sedentary habits and familiar hyper-trigliceridemia) and/or eating habits (hyper-caloric diets). It has been reported that triglycerides contents are associated with high blood viscosity (Rosenson *et al*., 2002), although measured with a viscometer at a single shear rate. In this regard, the complex rheological behavior of blood requires more suitable equipment and more detailed rheological tests, which are the motivations of this work. ANOVA analyses were made in order to compare the distribution of samples and all error values have been included.

2. Theoretical Section

2.1. The BMP constitutive equation

This constitutive equation contains an evolution equation for structure modification (Fredrickson, 1970), written in terms of the fluidity φ (inverse viscosity) bounded by two characteristic fluidities: the zero strain-rate fluidity φ_0 and the high-strain rate fluidity φ_∞. It involves a term for structure changes which is proportional to the viscous dissipation and a kinetic constant k, and another term for structure reformation proportional to a characteristic frequency λ^{-1}. This equation is coupled dynamically to a well-established non-linear objective rheological equation of state, the upper-convected Maxwell equation:

$$\frac{d\varphi}{dt} = \frac{(\varphi_0 - \varphi)}{\lambda} + k(\varphi_\infty - \varphi)\tau : D, \tag{1}$$

$$\tau + \delta(r, t)\overset{\nabla}{\tau} = \frac{\underline{\underline{D}}}{\varphi(r, t)}. \tag{2}$$

In Eqs. (1) and (2), τ is the stress tensor, $\underline{\underline{D}}$ is the rate of strain tensor, $\overset{\nabla}{\tau}$ is the upper convected derivative of the stress tensor, δ is a structure-dependent relaxation time $\delta = (G_0\varphi_0)^{-1}$, and G_0 is the elastic modulus. Eqs. (1) and (2) involve an underlying process of structure breakage and reformation, analogous to reversible kinetics with two rate constants, λ^{-1} and k. When the flow strength is high, the breakage process dominates and the viscosity level attains values near φ_∞^{-1}, while in the case of slow flows, the reformation process dominates with characteristic viscosity φ_0^{-1}. These coupled equations can predict primary creep or yield stress, a shear thinning or shear-thickening viscosity and elastic responses under unsteady-state flows, including thixotropy. For simple shear flow, Eqs. (1) and (2) become:

$$\frac{d\varphi}{dt} = \frac{(\varphi_0 - \varphi)}{\lambda} + k(\varphi_\infty - \varphi)\tau_{12}\dot{\gamma}, \tag{3}$$

$$\tau_{12} + \frac{1}{G_0\varphi}\frac{d\tau_{12}}{dt} - \frac{\tau_{22}\dot{\gamma}}{G_0\varphi} = \frac{\dot{\gamma}}{\varphi}, \tag{4}$$

$$N_1 + \frac{1}{G_0\varphi}\frac{dN_1}{dt} = \frac{2\tau_{12}\dot{\gamma}}{G_0\varphi}, \tag{5}$$

$$N_2 + \frac{1}{G_0\varphi}\frac{dN_2}{dt} = 0. \tag{6}$$

Here, τ_{12} is the shear stress, $\dot{\gamma}$ is the shear rate, N_1 and N_2 are the first and second normal-stress differences.

For steady simple-shear flow, the time derivatives become zero, and upon combination of Eqs. (3) and (4), a quadratic equation for the fluidity is obtained. The non-negative root gives the steady-state fluidity:

$$\varphi(\dot{\gamma}) = \frac{1}{2}\left[-(k\lambda\dot{\gamma}^2 - \varphi_0) + \left((k\lambda\dot{\gamma}^2 - \varphi_0)^2 + 4k\lambda\dot{\gamma}^2\varphi_\infty\right)^{\frac{1}{2}}\right]. \tag{7}$$

The shear viscosity is readily obtained:

$$\eta(\dot{\gamma}) = \frac{\left[(\eta_0 k\lambda\dot{\gamma}^2 - 1) + \left((\eta_0 k\lambda\dot{\gamma}^2 - \varphi_0)^2 + 4k\lambda\dot{\gamma}^2\left(\frac{\eta_0^2}{\eta_\infty}\right)\right)^{\frac{1}{2}}\right]}{2k\lambda\left(\frac{\eta_0}{\eta_\infty}\right)\dot{\gamma}^2}. \tag{8}$$

Complex fluids, such as human blood, present a spectrum of relaxation times, which is necessary to be accounted for in the model. A plausible generalization to include the spectrum is the summation of stress contributions of the

solvent (plasma) and various modes corresponding to different structures under flow. This concept can be expressed as follows:

$$\tau = \sum_{i=1}^{N} \tau_i + 2\eta_s D\,, \tag{9}$$

where η_s is the plasma viscosity and the stress contribution reflects the presence of various structures in the blood. The viscosity in turn for the multi-mode model may be expressed as:

$$\eta(\dot{\gamma}) = \sum_{i=1}^{N} \eta_i(\dot{\gamma})$$

$$= \sum_{i=1}^{N} \frac{\left[(\eta_{0i}k_i\lambda_i\dot{\gamma}^2 - 1) + \left((\eta_{0i}k_i\lambda_i\dot{\gamma}^2 - 1)^2 + 4k_i\lambda_i\dot{\gamma}^2\left(\frac{\eta_{0i}^2}{\eta_{\infty i}}\right)\right)^{\frac{1}{2}}\right]}{2k_i\lambda_i\dot{\gamma}^2\left(\frac{\eta_{0i}}{\eta_{\infty i}}\right)}, \tag{10}$$

$$\eta(\dot{\gamma}) = \sum_{i=1}^{N} \eta_i(\dot{\gamma})$$

$$= \sum_{i=1}^{N} \frac{\left[(\eta_{0i}\beta_i\lambda_i\dot{\gamma}^2 - 1) + \left((\eta_{0i}\beta_i\lambda_i\dot{\gamma}^2 - 1)^2 + 4\beta_i\lambda_i\dot{\gamma}^2\left(\frac{\eta_{0i}^2}{\eta_{\infty i}}\right)\right)^{\frac{1}{2}}\right]}{2\beta_i\dot{\gamma}^2\left(\frac{\eta_{0i}}{\eta_{\infty i}}\right)}. \tag{11}$$

Eq. (10) can be expressed as Eq. (11), we introduced a new parameter "β" that is defined as multiplication of k and λ constants.

2.2. Material properties

The BMP model was selected in this study due to its ability to predict the rheological behavior of structured fluids such as worm-like micellar solutions, dispersions of lamellar liquid crystals and associative polymers. In addition, the model reproduces the flow curve of shear-thinning and shear-thickening fluids, *i.e.*, a Newtonian plateau at low and high shear rates and the intermediate power law region for viscosity, non-vanishing normal-stress differences. It also gives a reasonable description of the elongational viscosity and stress relaxation and start-up curves, thixotropy and shear banding flow (Bautista *et al*., 1999; 2000; 2002; Manero *et al*., 2002; Calderas *et al*., 2009; Herrera *et al*., 2009; 2010; Soltero *et al*., 1999). Analytical solutions for a variety of flows are obtained due to its simplicity as compared to more complex models (Acierno *et al*., 1976; de Kee *et al*., 1994; Giesekus, 1966; 1982; 1984). Furthermore, the five parameters of the model are related to the fluid properties and can be estimated from independent rheological experiments in steady and unsteady state (Löffler *et al*., 2005). The viscosities η_0, η_∞ can be obtained from the low and high-shear-rate plateau in steady shear measurements. The modulus (G_0) can be obtained by oscillatory shear measurements or from instantaneous stress relaxation experiments. The agreement between the values of G_i obtained from these two experiments is within 10%. BMP constants λ and k are defined as characteristic time for structure built up and a kinetic constant for destruction of structure respectively (Bautista *et al*., 1999). The structural relaxation time λ can be estimated from the intercept of the stress relaxation times at long times after cessation of steady shear flow. The kinetic constant k, in turn, can be evaluated from the stress growth upon inception of shear flow (Soltero *et al*., 1999).

2.3. Oscillatory flow

In small deformation flows, the BMP equation reduces to the linear Maxwell model. In small amplitude oscillatory flow, the multimode version of the model renders the well-known expressions of storage and loss moduli.

$$G'(\omega) = \sum_{i=1}^{N} G_i \frac{\omega^2\lambda_i^2}{1+\omega^2\lambda_i^2}\,, \tag{12}$$

$$G''(\omega) = \sum_{i=1}^{N} G_i \frac{\omega\lambda_i}{1+\omega^2\lambda_i^2}\,. \tag{13}$$

Provided that the zero strain rate viscosity is:

$$\eta_{0i} = \sum_{i=1}^{N} G_i\lambda_i\,. \tag{14}$$

In the following section, results under steady-state flow, oscillatory flows are provided in blood samples with various cholesterol concentrations.

2.4. Mathematical modeling

The BMP model can reproduce the shear thinning behavior and elastic and viscous modulus of human blood under oscillatory deformations. We are considering the general model (BMP) with simplifications for different flow conditions*;* in the linear viscoelastic regime it reduces to the Maxwell model, provided that the parameters of the model are the same for both flow modes (oscillatory and continuous simple shear). The linear viscoelastic response was modeled with the multi-mode Maxwell model, expressed in terms of elastic and viscous moduli. This model contains specific parameters which represent characteristic values of relaxation time and moduli. These parameters were calculated for each sample using nonlinear regression data of corresponding oscillatory tests. Experimental results and modeling are used to explain the rheological behavior of the investigated samples.

The viscosity curve presents three different zones. The first one is located at low shear rate where erythrocytes remain close to each other, the second one at moderate shear rate wherein the erythrocytes are oriented in the flow direction and the last one at high shear rate, where

the erythrocytes are completely deformed and oriented. As shown later, each disaggregation processes can be described by one mode of the BMP model.

Among other models or approaches intended to describe the rheological behavior of blood, the Quemada model has been reported to represent the rheological behavior under shear-flow of blood samples (Marcinkowska-Gapińska *et al*., 2007). The model is based on five parameters: η_∞ is the viscosity at high shear rate, k_0 is the maximum volume fraction for zero shear rate, k_∞ is the maximum volume fraction for infinite shear rate, γ_c is characteristic rate of rouleaux formation/degradation and Hct is the hematocrit. In addition, the Carreau model has also been reported to describe the rheological behavior of blood under shear flow (Johnston *et al*., 2004).

3. Experimental Section

3.1. Rheological characterization

Rheological tests were performed in a controlled stress rheometer (AR-G2, TA® instruments) equipped with a double concentric cylinder fixture adapted for 5 mL samples. The concentric cylinders geometry was used because it is appropriate to low viscosity fluids, it keeps a uniform temperature preventing evaporation (a water seal was used) and the velocity gradient in the gap is nearly constant. In the parallel plates, on the other hand, a correction is needed due to the non-homogeneus radial dependence of the shear rate. In addition the gap in this geometry needs to be adjusted for each sample. The accuracy and reproducibility of rheological measurements can be affected by the tendency of blood cells to sediment, and by sample confinement size and geometry (Li *et al*., 2006). This was minimized by performing the measurements right after extraction and avoiding the use of the cone and plate geometry (it is not recommended for suspensions due to the aspect ratio effects of the red cells and gap). All measurements were performed under increasing and decreasing steady state shear rate protocols *i.e.* each viscosity point was taken under steady state (< 0.5% variation) time to reach steady state varies depending on the applied shear rate, but always longer than one minute . All measurements were confirmed in increasing and decreasing steady state shear rate protocols *i.e.* each viscosity point was taken in steady state (< 0.5% variation) and the time to reach steady state varies depending on the shear rate applied but in no case was set under 1 minute. The first step in all rheological tests is the application of pre-shearing with a shear rate of $\dot{\gamma} = 1\ s^{-1}$ to homogenize the proteins in the plasma and red blood cells, in a period of one minute. Simple-shear tests were performed from $\dot{\gamma} = 1\ s^{-1}$ to $\dot{\gamma} = 300\ s^{-1}$. The steady state for a given applied shear stress was attained past the initial transients for each value of stress, with a waiting time enough to obtain the time independent curve. Oscillatory tests were performed in a frequency range from $\omega = 1$ rad s^{-1} to $\omega = 300$ rad s^{-1} in the linear viscoelastic range. The linear viscoelastic range was identified by performing a strain amplitude sweeps at constant stress. The temperature was always kept at 37°C emulating the conditions of blood within the human body.

3.2. Microscopy

The microscopy study was carried out with blood adding EDTA in tubes. When the EDTA anticoagulant is used, a drop of a specimen is placed on a flat surface and a clean coverslip with smooth edges held at about a 45º tilt is used to spread the drop to produce a uniform film (Löffler *et al*., 2005). A microscope E2000LED MV Series Nikon® with a digital camera was used, with a total magnification of 1000 x.

4. Results and Discussion

4.1. Continuous simple-shear flow

Fig. 1 shows the simple-shear viscosity of samples disclosed in Table 1. The sample with the lowest cholesterol level shows an initial quasi-Newtonian region followed by shear-thinning at high shear rates (> 10 s^{-1}). The quasi-plateau asymptote increases with cholesterol content and a more pronounced shear-thinning region appears at low shear-rates for the samples with the highest cholesterol content (H1-H6). Red cells aggregation is an interesting phenomenon in hemo-rheology, influencing the in-vitro rheological properties of blood. Plasmatic levels of total cholesterol and triglycerides usually modify the degree of aggregation. At low shear rates, the zero shear-rate viscosity is strongly dependent on RBC aggregation; an enhanced RBC aggregation caused by the increasing cholesterol content leads to the apparition of yield stresses in these samples. At moderate shear rates, RBC tend to separate and disaggregate, inducing shear thinning. At high

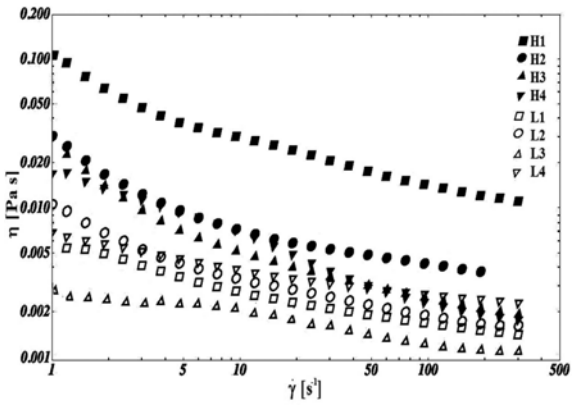

Fig. 1. Viscosity of blood samples with various cholesterol levels under simple shear flow.

Table 1. Clinical data for the blood samples used in this study. Samples H1-H6 have high cholesterol levels and samples L1-L6 lie within the average range. ANOVA analysis $\alpha < 0.05$.

Sample	TC (mg/dL)	GC (mg/dL)	HDL (mg/dL)	LDL (mg/dL)	Fibrinogen (mg/dL)	Hct (%)
H1	400 ± 12.3	250 ± 6.1	35.5 ± 0.5	135.5 ± 3.2	284 ± 7.1	48.2 ± 1.1
H2	268 ± 3.7	157 ± 2.6	36.1 ± 0.9	130.8 ± 3.1	278 ± 6.9	47.9 ± 1.0
H3	250 ± 3.5	187 ± 3.4	38.2 ± 0.7	139.4 ± 3.4	273 ± 6.6	48.0 ± 1.1
H4	290 ± 4.0	160 ± 3.2	40.6 ± 1.0	149.1 ± 3.6	278 ± 6.8	47.8 ± 1.0
H5	300 ± 4.1	190 ± 3.3	38.9 ± 0.7	136.0 ± 3.3	286 ± 7.1	47.9 ± 1.0
H6	310 ± 4.3	197 ± 3.6	36.8 ± 0.6	149.1 ± 3.6	285 ± 7.0	49.0 ± 1.2
L1	187 ± 3.6	180 ± 3.3	48.8 ± 1.1	159.1 ± 4.0	288 ± 7.2	48.7 ± 1.1
L2	164 ± 3.1	122 ± 2.2	46.7 ± 1.0	148.9 ± 3.6	275 ± 6.4	48.8 ± 1.0
L3	109 ± 2.1	130 ± 2.3	47.6 ± 0.9	146.8 ± 3.5	270 ± 6.5	49.0 ± 1.2
L4	180 ± 3.5	145 ± 2.6	40.6 ± 0.8	144.5 ± 3.5	278 ± 6.5	47.9 ± 1.0
L5	150 ± 2.8	130 ± 2.2	44.9 ± 1.0	153.6 ± 3.0	285 ± 7.0	48.5 ± 1.1
L6	165 ± 3.2	125 ± 2.2	39.8 ± 0.7	154.8 ± 3.1	289 ± 7.2	48.6 ± 1.1

*ANOVA, $\alpha < 0.05$.

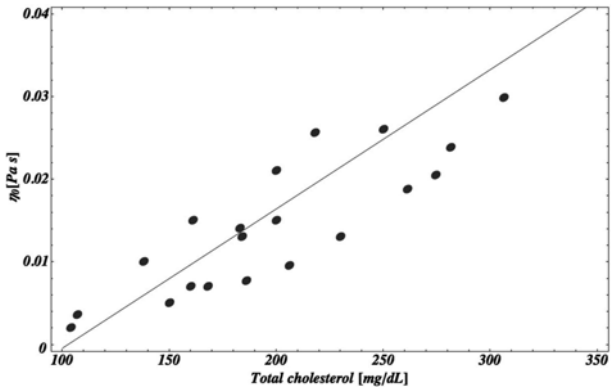

Fig. 2. Blood viscosity as a function of cholesterol content at $\dot{\gamma} = 1\ s^{-1}$. The line shows a linear regression of data.

shear rates, RBC deformation occurs and the cells orient in the flow direction, attaining values in the range of the plasma viscosity. This is the reason why we choose to correlate the zero shear rate viscosity with total cholesterol content in Fig. 2. These curves evidence the ability of total cholesterol to promote cell aggregation (Saldahna *et al.*, 2011); these cell aggregates are transient and easily disrupted by flow. At the surface of the cell membranes, molecules with polar characteristics (such as sialic acid) induce a negative charge to the membrane and hence the interaction between the two cells is repulsive, but nonetheless fibrinogen neutralize these charges.

In this work, donors presented only metabolic syndrome (high plasmatic levels of total cholesterol and triglycerides), but they do not present hyper-gammaglobulinemia or hyper-proteinemia, consequently the occurrence of the rouleaux structure is not likely (Ford, 2013). Presumably, molecules of cholesterol promote lower repulsion and thus cell aggregation; consequently, models for red blood cell aggregation (RBC) consider bridging and depletion. In the bridging model, red cell aggregation is proposed to occur when the bridging forces due to the adsorption of macromolecules onto adjacent cell surfaces exceed disaggregating forces due to electrostatic repulsion, membrane strain and mechanical shearing (Brooks, 1973, 1988; Chien *et al*., 1973, 1987; Snabre and Mills, 1985; Solheim *et al*., 2004). This model is similar to others which propose cell interactions like agglutination, except that the proposed adsorption energy of the macromolecules is much smaller, in accord to the relative weakness of these forces. In contrast, the depletion model proposes quite the opposite. In this model, RBC aggregation is explained to occur as a result of a lower localized protein or polymer concentration near the cell surface compared to the suspending medium (*i.e.* relative depletion near the cell surface). This exclusion of macromolecules near the cell surface leads to an osmotic gradient and thus depletion interaction (Snabre *et al*., 1985). As with the bridging model, disaggregation forces are electrostatic repulsion, membrane strain and mechanical shearing (Bäumler *et al*., 1996).

It is evident that cholesterol content plays an important role in modifying the viscosity of blood. In Fig. 1, the sample with the highest level of total cholesterol has the highest viscosity (H1) and the sample with the lowest level of cholesterol displays the lowest viscosity of all samples (L3). Samples with high cholesterol levels (H1-H6) show a similar trend as a yield stress fluid with viscosity increasing as shear rate decreases. Blood with high cholesterol levels causes arteries clogging in the long run and also causes the heart to work harder to move a more viscous fluid. However, the relation between cholesterol content and viscosity is not a simple one. Viscosity does not increase linearly with cholesterol content although it is an important contributor to build up viscosity as shown in

Fig. 2, where viscosity values taken at 1 s^{-1} are plotted as a function of the cholesterol content in 20 blood samples. Fig. 2 shows an evident tendency of increasing blood viscosity with total cholesterol content. It is important to mention that the larger differences in blood viscosity are observed at low shear rates (zero shear rate viscosity). For this reason, the viscosity values depicted in Fig. 2 are taken at 1 s^{-1}. At shear rates of about 100 s^{-1}, curves tend to overlap and this does not allow a proper appreciation of the influence of cholesterol on blood viscosity. It is then very important to evaluate the viscosity along a wide range of shear rates and not only at a single shear rate.

Triglycerides (TG) content in blood presents no direct influence in blood viscosity as in the case of cholesterol. This can be observed in Table 1 and Fig. 1; for example, sample L1 has the highest TG level in the low-cholesterol samples (L1-L6) even higher than in samples H2 and H4. However, sample L1 is one of the samples with the lowest viscosity (see Fig. 1). Another example is sample H3, which has a high TG level compared with the other samples of the low cholesterol level set (H1-H6). Nevertheless, sample H3 has the lowest viscosity values of all samples (in the shear rate range 3-20 s^{-1}) of the low cholesterol set and this is determined by its relative low cholesterol content and not by its high TG value (see Table 1).

4.2. Small amplitude oscillatory shear flow (SAOS)

Fig. 3 shows the complex viscosity versus oscillatory frequency. It is interesting to note that the viscosity decrease observed in the continuous shear-flow experiments is absent here (the Cox-Merz rule is not followed). Almost all samples show a viscosity plateau, which reinforces the hypothesis that cholesterol increases the transient cell interactions. These interactions are not disrupted using small amplitude oscillatory shear, indicating that these aggregations are stable to this flow. Again, the sample with the highest cholesterol content shows the highest complex viscosity and they almost overlap (H1-H6). Two sets of curves are then suggested, those with high levels of cholesterol (H1-H6) and those with low levels of cholesterol (L1-L6).

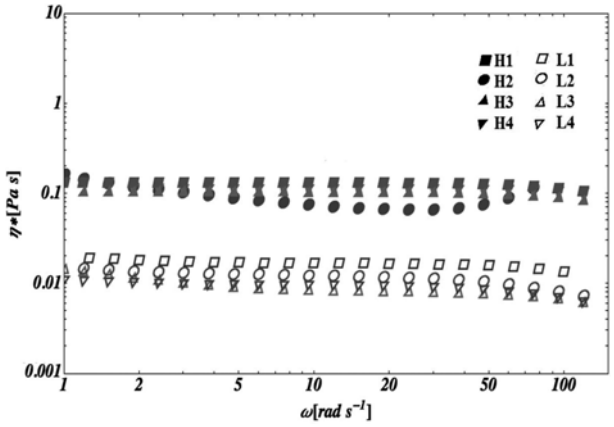

Fig. 3. Complex viscosity as a function of frequency measured under a SAOS test for various samples.

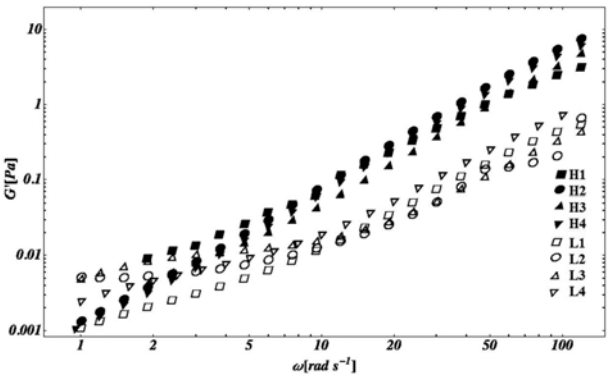

Fig. 4. Elastic modulus as a function of frequency under a SAOS test for blood samples with various cholesterol levels.

Fig. 4 depicts the elastic modulus against oscillatory frequency, wherein two different behaviors are observed. The high- cholesterol samples (H1-H6) show larger elasticity and in general, they show similar slopes at low frequency, with the exception of the H1 sample, which shows a slope change at low frequency. This terminal behavior is indicative of strong interactions in heterogeneous systems, also observed in other complex fluids (Calderas *et al*., 2009; Marcinkowska-Gapińska *et al*., 2007; Baskurt and Meiselman, 2013) and presumably is ascribed to the combined effect of high cholesterol and triglycerides content. These two associated structures cause the formation of a strong interacting network by cell aggregation and complex molecular interactions. This is still a speculative issue since it is difficult to find donors with the suitable cholesterol and triglycerides contents for a full analysis. Samples with low cholesterol levels depict a different behavior with an evident slope change at intermediate frequencies (20 s^{-1}) and lower elasticity. Sample L1 shows a slight slope change attributed to the cholesterol content (L1 has the highest cholesterol level in this group).

Fig. 5 shows G' against G'' constructed using the linear viscoelastic data of the blood samples. Two sets of curves are clearly distinguishable, one for high cholesterol levels (H1-H4) and another one for low levels (L1-L6). Since blood is predominantly viscous along the frequency range, both sets of curves lie in the region of viscous behavior above the crossover line ($G' = G''$). To illustrate the suitability of this representation, it is interesting to note that sample L3 lies apart from the low cholesterol set at low frequency. This behavior is attributed to the high triglyceride content of this sample combined with low cholesterol levels. Sample H1 also lies outside of the group of curves having high cholesterol content, attributed to its very high cholesterol content.

Fig. 6 depicts SAOS data in the form of η'' versus η'

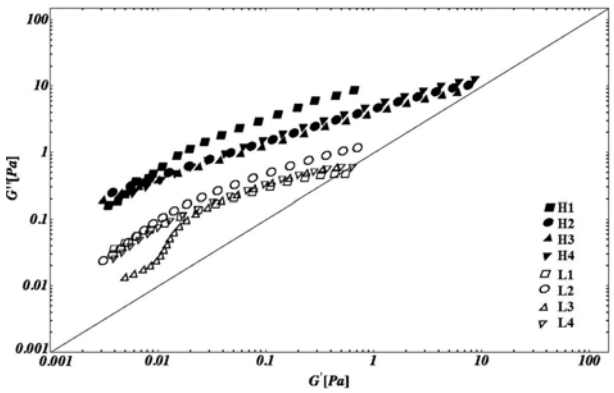

Fig. 5. Storage modulus versus loss modulus from the SAOS data for blood with different cholesterol levels. The straight line represent the equality $G'' = G'$.

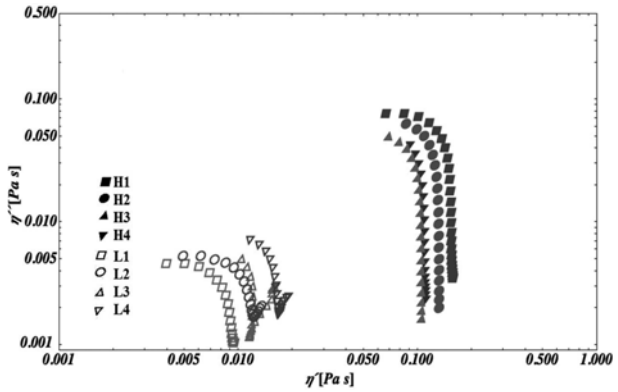

Fig. 6. The imaginary part versus the real part of dynamic viscosity from SAOS data for samples with different cholesterol levels.

(imaginary and real parts of the complex viscosity). Again, two sets of curves are observed, quite separated each other. The dominant relaxation mechanism is also clearly observed (maximum in the curves). However the set of curves with low cholesterol levels, except L1, depicts two characteristic relaxation times (curves exhibit a minimum and subsequently spikes, ascribed to a second relaxation process). Sample L1 does not exhibit the second relaxation which is in common to the high cholesterol samples. This representation is useful to show that the cholesterol layer screens interactions among the erytocytes that lead to a single dominant relaxation mechanism. Samples with two relaxation mechanisms exhibited by the Cole-Cole plot have been reported in other systems (such as polymer blends) in which the second relaxation mechanism is attributed to non-homogeneities in the system (Giesekus, 1966; Li *et al*., 2006).

4.3. Microscopy

The slide glass preparation was performed according with the hematological smear technique (Löffler *et al.*, 2005). Optical microscopy tests for two samples with high

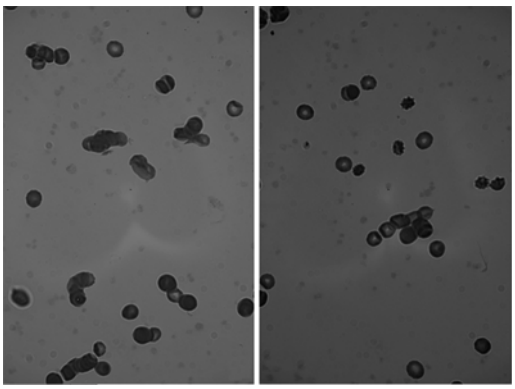

Fig. 7. Blood smears of (a) high (H1 left) and (b) low (L3 right) cholesterol sample.

(H1) and low (L3) cholesterol levels are shown in Fig. 7. Samples with high total cholesterol and triglycerides levels show higher erythrocyte aggregations, reinforcing the hypothesis of cholesterol as a promoter of cell aggregation (Fig. 7a), in accord to the complex rheological behavior observed in the previous section. In contrast, the sample with low cholesterol content shows more dispersed erythrocytes and few cell aggregations (Fig. 7b).

4.4. Rheological modeling

Caram *et al*. (2006) have reported the use of the multimode BMP model to predict the rheological behavior of commercial hydrophobic alkali soluble emulsion (HASE) in small-amplitude oscillatory, steady, and unsteady simple shear flows. The same procedure to model the experimental data under oscillatory and steady shears flow experiments is employed here, using the multimodal Maxwell and BMP models, respectively. Also, we use the models by Quemada and Carreau model to demonstrate the models ability to describe the rheological behavior of human blood under shear flow. Quemada and Carreau models also describe the shear thinning behavior of whole human blood quite well, but they do not include predictions of blood viscoelasticity (Campo-Deaño *et al*., 2013).

Fig. 8 depicts the models predictions under simple shear flow for sample L3. It is important to note deviations of predictions from the data at low shear rates, implying the presence of additional modes. However, the model was kept as simple as possible (correlation is below 5% error), but nevertheless, it describes these complex data in the low shear rate region comparatively better. Table 2 displays the model parameters used in the simulation.

Fig. 9 depicts the Maxwell model predictions with SAOS data for sample L3. It is important to note that predictions are in good agreement with data. Three modes were necessary to adequately predict the rheological behavior. Table 2 displays the model parameters used in the simulation. With high fibrinogen levels, yield stress phenomena are present in human blood; indeed, fibrinogen promotes

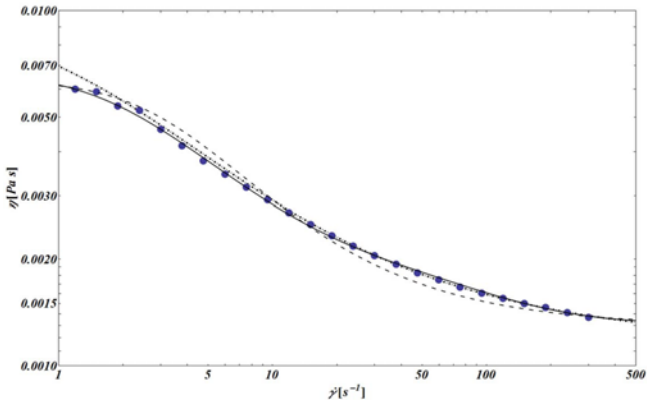

Fig. 8. BMP model (solid line) predictions, rheological data (dots), Quemada model (Dashdot line), and Carreau model (dashed line) for sample L3 under simple-shear flow.

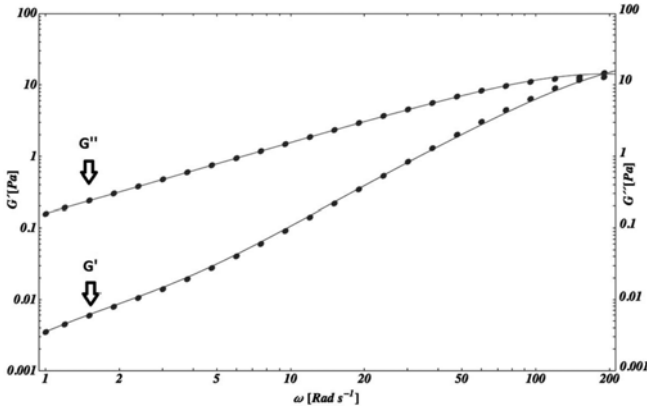

Fig. 9. Maxwell model (solid line) predictions and rheological data (dots) for sample L3 under linear oscillatory shear flow.

increasing interactions between cells leading to dimeric fibrinogen structures (Merrill *et al*., 1969). Jung *et al.* (2014) found an important relationship between a disaggregating shear stress (DSS) and fibrinogen concentration. DSS increase as a function of fibrinogen concentration from 250 mPa to 1200 mPa with 200 mg/dL to 600 mg/dL respectively. It is important to note that fibrinogen concentrations of all samples lie inside the normal range, for both high and low groups remain almost constant (281.3 ± 6.18 mg/dL).

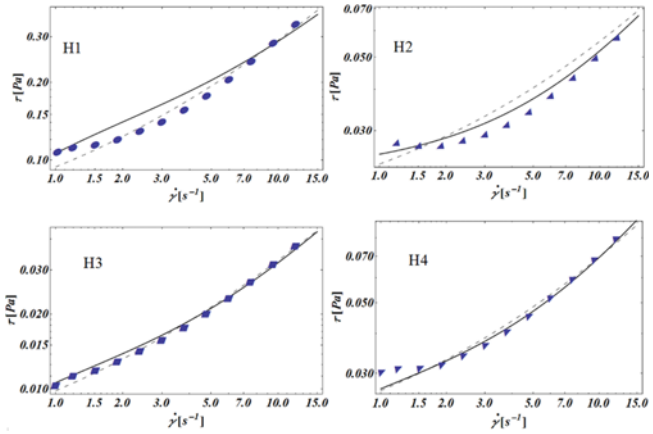

Fig. 10. Predictions of the Casson (dashed line) and BMP (solid line) models using H1-H4 samples (highest total cholesterol and triglycerides contents, dots) at low shear rates.

Although high concentrations of total cholesterol and triglycerides increase interactions between cells, the mechanism by which fibrinogen induces links between two adjacent cells is different. Fig. 10 depicts predictions of the yield stress calculated with the Casson and BMP models, to illustrate the close relationship of yield stress and high cholesterol contents. A linear correlation is found Fig. 11, revealing that the yield stress level is proportional to the number of links between cells (Merrill *et al*., 1969). With normal fibrinogen levels, high total cholesterol and triglycerides contents enhance the value of the yield stress. The Casson and BMP models predict the yield stress values adequately. The BMP model can predict yield stress values as well as Casson model does Fig. 10. The parameters for the simulation and the values of the yield stress for each model are presented in Table 3. Yield stress with the BMP model can be calculated when $\varphi_0 = 0$, the model predicts a yield stress value $\sigma_y = (k\lambda\varphi_\infty)^{-1/2}$ Calderas *et al.* (2013) or in other terms $\sigma_y = (\beta\varphi_\infty)^{-1/2}$.

Casson model parameters considered for human blood are the following: yields stress σ_0 (Pa), Casson viscosity K_0 (Pa·s) and the extra terms η_F and Φ are hematocrit independent Casson blood viscosity and volume fraction

Table 2. BMP, Quemada, and Carreau model parameters used in the simulations shown in Fig. 9 (sample L3). Parameters units of BMP model β (s/Pa), η_{0i} and η_∞ (Pa·s). Parameters units for Carreau model η_0 and η_∞ (Pa·s), λ (s) and n dimensionless. Parameters of Quemada model η_∞ (Pa·s), $\dot{\gamma}_c'$ (1/s), k_0 and k_∞ are dimensionless.

Quemada		Carreau		Bautista-Manero-Puig				Multimodal Maxwell Model			
η_∞	0.00108	η_0	0.00638	η_i	$i=1$	$i=2$	$i=3$	G_i	$i=1$	$i=2$	$i=3$
					0.00534	0.001	0.000994		28.5	0.37	0.01
k_0	8	η_∞	0.0013	β_i	2.23	0.062	0.001	λ_i	0.0052	0.03	0.79
k_∞	0.13	λ	0.338								
γ_c'	2.44	n	0.1	$\eta_{\infty i}$	2.3×10^{-4}	2.3×10^{-4}	2.3×10^{-4}				

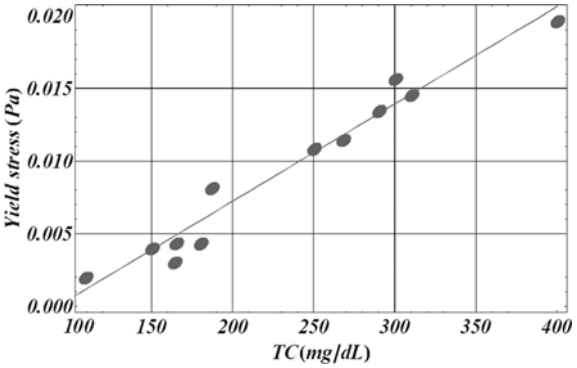

Fig. 11. Yield stress as a function of total cholesterol of 12 samples calculated with the Casson model.

Table 3. Yield stress values and parameters for the BMP and Casson models used in Fig. 11. Casson model units σ_0 (Pa), K_0 (Pa·s). BMP model units β (s/Pa), φ_∞ (1/Pa·s), and σ_0 (Pa).

	Model					
	Casson		BMP			
Sample	σ_0	K_0	β	η_∞	φ_∞	σ_0
H1	0.0396	0.01158	0.845	0.001	1000	0.034401
H2	0.0134	0.00217	1.75	0.0009	1111.111	0.022678
H3	0.0134	0.00144	0.9	0.0006	1666.667	0.02582
H4	0.00376	0.00143	1.65	0.0015	666.667	0.003018

(hematocrit) respectively (Marcinkowska-Gapińska *et al*., 2007).

5. Conclusions

Human blood with various cholesterol levels was characterized under simple shear and oscillatory shear-flow experiments. Human blood behaves as a complex non-Newtonian fluid with pseudo-plastic characteristics. Cholesterol and triglycerides concentrations promote aggregation of erythrocytes with relatively high viscosity. Hematocrit differences were not significant in the samples. Although the cholesterol content-viscosity relation is not linear, there is an overall tendency of blood to become more viscous and pseudo-plastic as the cholesterol content increases, with similarities with a yield stress fluid behavior. Micrographs suggest that cell aggregation increases by cholesterol plasmatic levels. A high viscosity in the human blood involves problems such as retinal circulation, capillary occlusion and several circulation deceases. The complex rheological behavior of blood was adequately modeled using the multi-mode version of the Maxwell and BMP models, which facilitates the mathematical modeling of blood under more complex flow situations. Comparisons with predictions from other models for the same samples were also made. Results evidence the influence of total cholesterol and triglycerides on blood viscosity which induces red blood cell aggregation.

Acknowledgements

We acknowledge the support of Dr. Claudia Huesca Gomez from National Institute of Cardiology for samples and the support of the National Council of Science and Technology (CONACYT) for the scholarship 353344 and PAPIIT project from UNAM IN118414. Also we acknowledge the financial support from IIM-UNAM (Postdoctoral Grant) and the donors: Angelica Campos, Sabina Alvarez, Alicia Cortes, Jose Hurtado, Marisol Jardon, Alberto de la Cruz, Irasu Dander, Fausto Calderas, Luis Medina-Torres, Lucina Guerrero and Luis Ordaz.

References

Acierno, D., F.P. La Mantia, G. Marrucci, and G. Titomanlio, 1976, A non-linear viscoelastic model with structure-dependent relaxation times: I. Basic formulation, *J. Non-Newton. Fluid* **1**, 125-146.

Bautista, F., J.M. de Santos, J.E. Puig, and O. Manero, 1999, Understanding thixotropic and antithixotropic behavior of viscoelastic micellar solutions and liquid crystalline dispersions. I. The model, *J. Non-Newton. Fluid* **80**, 93-113.

Bautista, F., J.F.A. Soltero, J.H. Pérez-López, J.E. Puig, and O. Manero, 2000, On the shear banding flow of elongated micellar solutions, *J. Non-Newton. Fluid* **94**, 57-66.

Bautista, F., J.F.A. Soltero, E.R. Macias, and O. Manero, 2002, On the shear banding flow of wormlike micelles, *J. Phys. Chem. B* **106**, 13018-13026.

Baskurt, O.K. and H.J. Meiselman, 2013, Erythrocyte aggregation: Basic aspects and clinical importance, *Clin. Hemorheol. Micro.* **53**, 23-37.

Bäumler, H., E. Donath, A. Krabi, W. Knippel, A. Budde, and H. Kiesewetter, 1996, Electrophoresis of human red blood cells and platelets. Evidence for depletion of dextran, *Biorheology* **33**, 333-351.

Brooks, D.E., 1973, The effect of neutral polymers on the electrokinetic potential of cells and other charged particles: III. Experimental studies on the dextran/erythrocyte system, *J. Colloid Interf. Sci.* **43**, 700-713.

Brooks, D.E., 1988, Mechanism of red cell aggregation. In *Blood Cells, Rheology, and Aging*, Springer Berlin Heidelberg, pp. 158-162.

Calderas, F., A. Sanchez-Solis, A. Maciel, and O. Manero, 2009, The Transient Flow of the PET-PEN-Montmorillonite Clay Nanocomposite, *Macromol. Symp.* **283**, 354-360.

Calderas, F., E.E. Herrera-Valencia, A. Sanchez-Solis, O. Manero, L. Medina-Torres, A. Renteria, and G. Sanchez-Olivares, 2013, On the yield stress of complex materials, *Korea-Aust. Rheol. J.* **25**, 233-242.

Campo-Deaño, L., R.P. Dullens, D.G. Aarts, F.T. Pinho, and N.S. Oliveira, 2013, Viscoelasticity of blood and viscoelastic blood analogues for use in polydymethylsiloxane in vitro models of

the circulatory system, *Biomicrofluidics* **7**, 034102.
Caram, Y., F. Bautista, J.E. Puig, and O. Manero, 2006, On the rheological modeling of associative polymers, *Rheol. Acta* **46**, 45-57.
Chien, S., R.J. Dellenback, S. Usami, D.A. Burton, P.F. Gustavson, and V. Magazinovic, 1973, Blood volume, hemodynamic, and metabolic changes in hemorrhagic shock in normal and splenectomized dogs, *Am. J. Physiol.* **225**, 866-879.
Chien, S. and L.A. Sung, 1987, Physicochemical basis and clinical implications of red cell aggregation, *Clin. Hemorheol.* **7**, 71-91.
de Kee, D. and C.F. Chan Man Fong, 1994, Rheological properties of structured fluids, *Polym. Eng. Sci.* **34**, 438-445.
Esteridge, B.H., A.P. Reynolds, and N.J. Walters, 2000, *Basic Medical Laboratory Techniques*, Cengage Learning, pp. 127.
Ford, J., 2013, Red blood cell morphology, *Int. J. Lab. Hematol.* **35**, 351-357.
Fredrickson, A.G., 1970, A model for the thixotropy of suspensions, *AIChE J.* **16**, 436-441.
Giesekus, H., 1966, Die elastizität von flüβigkeiten, *Rheol. Acta* **5**, 29-35.
Giesekus, H., 1982, A simple constitutive equation for polymer fluids based on the concept of deformation-dependent tensorial mobility, *J. Non-Newton. Fluid* **11**, 69-109.
Giesekus, H., 1984, On configuration-dependent generalized Oldroyd derivatives, *J. Non-Newton. Fluid* **14**, 47-65.
Herrera, E.E., F. Calderas, A.E. Chávez, O. Manero, and B. Mena, 2009, Effect of random longitudinal vibrations on the Poiseuille flow of a complex liquid, *Rheol. Acta* **48**, 779-800.
Herrera, E.E., F. Calderas, A.E. Chávez, and O. Manero, 2010, Study on the pulsating flow of a worm-like micellar solution, *J. Non-Newton. Fluid* **165**, 174-183.
Högman, C.F., 1999, Storage of blood components, *Curr. Opin. Hematol.* **6**, 427-431.
Högman, C.F. and H.T. Meryman, 1999, Storage parameters affecting red blood cell survival and function after transfusion, *Transfus. Med. Rev.* **13**, 275-296.
Johnston, B.M., P.R. Johnston, S. Corney, and D. Kilpatrick, 2004, Non-Newtonian blood flow in human right coronary arteries: steady state simulations, *J. Biomech.* **37**, 709-720.
Jung, J., B.K. Lee, and S. Shin, 2014, Yield shear stress and disaggregating shear stress of human blood, *Korea-Aust. Rheol. J.* **26**, 191-198.
Li, R., W. Yu, and C. Zhou, 2006, Rheological characterization of droplet-matrix versus co-continuous morphology, *J. Macromol. Sci. B* **45**, 889-898.
Lerman-Garber, I., J.A. Sepulveda-Amor, R. Tapia-Conyer, C. Magos-Lopez, G. Cardoso-Saldana, J. Zamora-Gonzalez, and C. Posadas-Romero, 1993, Cholesterol levels and prevalence of hypercholesterolemia in Mexican children and teenagers, *Atherosclerosis* **103**, 195-203.
Longster, G.H., T. Buckley, J. Sikorski, and L.A. Tovey, 1972, Scanning electron microscope studies of red cell morphology, *Vox Sang.* **22**, 161-170.
Loffler, H., J. Rastetter, T. Haferlach, and H. Begemann, 2005, *Atlas of Clinical Hematology 6th Ed*., Springer, pp. 4.
Manero, O., F. Bautista, J.F.A. Soltero, and J.E. Puig, 2002, Dynamics of worm-like micelles: the Cox–Merz rule, *J. Non-Newton. Fluid* **106**, 1-15.
Marcinkowska-Gapińska, A., J. Gapinski, W. Elikowski, F. Jaroszyk, and L. Kubisz, 2007, Comparison of three rheological models of shear flow behavior studied on blood samples from post-infarction patients, *Med. Biol. Eng. Comput.* **45**, 837-844.
Merrill, E.W., C.S. Cheng, and G.A. Pelletier, 1969, Yield stress of normal human blood as a function of endogenous fibrinogen, *J. Appl. Physiol.* **26**, 1-3.
Rosenson, R.S., S. Shott, and C.C. Tangney, 2002, Hypertriglyceridemia is associated with an elevated blood viscosity Rosenson: triglycerides and blood viscosity, *Atherosclerosis*, **161**, 433-439.
Saldanha, C., J. Loureiro, C. Moreira, and J. Silva, 2011, Behaviour of human erythrocyte aggregation in presence of autologous lipoproteins, *Biochem. Res. Int.* **2012**, 261736.
Schmid-Schönbein, H., P. Gaehtgens, and H. Hirsch, 1968, On the shear rate dependence of red cell aggregation in vitro, *J. Clin. Invest.* **47**, 1447-1454.
Snabre, P. and P. Mills, 1985, Effect of dextran polymer on glycocalyx structure and cell electrophoretic mobility, *Colloid Polym. Sci.* **263**, 494-500.
Solheim, B.G., O. Flesland, J. Seghatchian, and F. Brosstad, 2004, Clinical implications of red blood cell and platelet storage lesions: an overview, *Transfus. Apher. Sci.* **31**, 185-189.
Soltero, J.F.A., F. Bautista, J.E. Puig, and O. Manero, 1999, Rheology of cetyltrimethylammonium p-toluenesulfonate-water system. 3. Nonlinear viscoelasticity, *Langmuir*, **15**, 1604-1612.
Thurston, G.B., 1972, Viscoelasticity of human blood, *Biophys. J.* **12**, 1205-1217.
Thurston, G.B., 1975, Elastic effects in pulsatile blood flow, *Microvasc. Res.* **9**, 145-157.